

Hindawi Publishing Corporation  
Journal of Nanomaterials  
Volume 2007, Article ID 94975, 5 pages  
doi:10.1155/2007/94975

## Research Article

# Morphology and Luminescence of Nanocrystalline Nb<sub>2</sub>O<sub>5</sub> Doped with Eu<sup>3+</sup>

Daniele Falcomer,<sup>1</sup> Adolfo Speghini,<sup>1</sup> Giulio Ibba,<sup>2</sup> Stefano Enzo,<sup>2</sup> Carla Cannas,<sup>3</sup>  
Anna Musinu,<sup>3</sup> and Marco Bettinelli<sup>1</sup>

<sup>1</sup> *Dipartimento Scientifico e Tecnologico, Università di Verona and INSTM, UdR Verona, Strada Le Grazie 15, 37134 Verona, Italy*

<sup>2</sup> *Dipartimento di Chimica, Università di Sassari and INSTM, UdR Sassari, Via Vienna 2, 07100 Sassari, Italy*

<sup>3</sup> *Dipartimento di Scienze Chimiche, Università di Cagliari and INSTM, UdR Cagliari, Complesso Universitario, S.S. 554, Bivio per Sestu, Monserrato, 09042 Cagliari, Italy*

Received 12 March 2007; Accepted 4 June 2007

Recommended by Wieslaw Strek

The synthesis of nanocrystalline Nb<sub>2</sub>O<sub>5</sub>:Eu<sup>3+</sup> has been achieved by using a Pechini procedure. The obtained materials are single-phase niobia with the orthorhombic structure, average crystallite size around 25 nm and average lattice strain of about 0.002. TEM images show that the particles are rectangular and reasonably isolated. The luminescence of the Eu<sup>3+</sup> ions in the niobia lattice is efficient and affected by a strong inhomogeneous broadening, due to an important disorder around the lanthanide ions.

Copyright © 2007 Daniele Falcomer et al. This is an open access article distributed under the Creative Commons Attribution License, which permits unrestricted use, distribution, and reproduction in any medium, provided the original work is properly cited.

## 1. INTRODUCTION

Luminescent niobate crystals activated with trivalent lanthanide ions (Ln<sup>3+</sup>) have been the subject of considerable attention in the past decades. In particular, lithium niobate (LiNbO<sub>3</sub>) has attracted huge interest as a valuable host for Ln<sup>3+</sup> ions, with important applications in the field of optoelectronics and light emitting devices [1]. Moreover, other niobates such as strontium barium niobate (Sr<sub>x</sub>Ba<sub>1-x</sub>Nb<sub>2</sub>O<sub>6</sub>) (SBN) and barium sodium niobate (BNN), activated with Ln<sup>3+</sup> ions, are very promising materials in the field of photorefractive memories [2] and linear and self-frequency converter solid state laser materials [3, 4]. It is important to note that in all these crystals the location of the Ln<sup>3+</sup> in the lattice is not obvious, as the trivalent lanthanide ions cannot easily replace the constitutional cations (Li<sup>+</sup>, Na<sup>+</sup>, Sr<sup>2+</sup>, Ba<sup>2+</sup>, Nb<sup>5+</sup>) due to clear size and/or charge mismatches. This location has been addressed by several studies where optical and/or structural techniques have been employed [5, 6]. Nevertheless, it is still a matter of debate whether the Ln<sup>3+</sup> can substitute for the smaller and higher charged Nb<sup>5+</sup> cation in a crystalline lattice [7]. One possible contribution to the solution of this problem is to verify if it is feasible to dope Ln<sup>3+</sup> ions in a lattice in which *only* the formally pentavalent niobium cations can be replaced, that is, Nb<sub>2</sub>O<sub>5</sub>. For this reason, we found it in-

teresting to investigate the synthesis and the structural properties of crystalline niobia (Nb<sub>2</sub>O<sub>5</sub>), doped with Eu<sup>3+</sup>. Moreover, although nanocrystalline niobia has been shown to be a valuable material finding applications as catalyst and sensor [8, 9], very scarce information is available on the preparation and spectroscopic investigation of nanocrystalline Nb<sub>2</sub>O<sub>5</sub> activated with lanthanide ions. For this reason, in this paper we report on the synthesis and characterization, and on the optical spectroscopy of Nb<sub>2</sub>O<sub>5</sub>:Eu<sup>3+</sup> in nanocrystalline form.

## 2. EXPERIMENTAL PROCEDURE

Nanocrystalline powders of Eu<sup>3+</sup> doped Nb<sub>2</sub>O<sub>5</sub> were prepared by a Pechini approach [10]. The molar ratio between the niobium and the Eu<sup>3+</sup> ions was 99:1. An appropriate amount of citric acid was first dissolved in hot water, then niobium ammonium oxalate (NAmOx), Eu(NO<sub>3</sub>)<sub>3</sub>, and polyethylene glycol (PEG) were added. The resulting solution was stirred for 10 minutes. The gel was obtained by drying the solution at 90°C for 2 days. The nanocrystalline powder was obtained by heat-treating the gel at 400°C for 2 hours and then at 600°C for 1 hour. The sample will be denoted as Nb<sub>2</sub>O<sub>5</sub>:Eu hereafter.

The powder X-ray diffraction (XRD) pattern of the Nb<sub>2</sub>O<sub>5</sub>:Eu sample was recorded overnight with a Bruker D8

diffractometer in the Bragg-Brentano geometry using Cu  $K_\alpha$  radiation ( $\lambda = 1.5418 \text{ \AA}$ ). The X-ray generator worked at a power of 40 kV and 40 mA and the goniometer was equipped with a graphite monochromator in the diffracted beam. The resolution of the instrument (divergent and antiscatter slits of  $0.5^\circ$ ) was determined using  $\alpha\text{-SiO}_2$  and  $\alpha\text{-Al}_2\text{O}_3$  standards free from the effect of reduced crystallite size and lattice defects. The powder patterns were analyzed according to the Rietveld method [11] using the program MAUD [12] running on a personal computer. It is worth to recall that the MAUD program takes into account precisely the instrument broadening and, under the selected assumption of isotropic peak broadening as a function of reciprocal space, performs the separation of the lattice strain contribution to the broadening from the reduced crystallite size. Relative agreement factors  $R_{wp}$  and  $R_B$  are generally reported to determine the ability of the implemented structural model in accounting for the experimental data, which are unavoidably affected by statistical noise due to the limited time of pattern collection.

Transmission electronic microscopy (TEM) images were obtained with a JEM 200CX working at 200 kV; selected area diffraction images were obtained with a camera length of 82 cm.

The 488.0 nm line of a Spectra-Physics Stabilite 2017 argon Laser was used to excite the luminescence and Raman spectra. The emission radiation was collected by using an optical fiber and dispersed with a Jobin-Yvon HR460 0.46 m monochromator equipped with a 150 lines/mm (for low-resolution luminescence spectra) or a 1200 lines/mm (for high-resolution luminescence and Raman spectra) grating. A suitable notch filter was employed to measure the Raman spectrum, in order to suppress the 488.0 nm Rayleigh radiation. Due to the notch filter, the Raman spectrum can be collected for Raman shifts higher than  $250 \text{ cm}^{-1}$ . An air cooled Jobin-Yvon Spectrum One CCD device was employed to detect the emission radiation. The resolution of the luminescence spectra is  $\pm 1 \text{ nm}$  for low-resolution luminescence spectra (560–730 nm range) and  $\pm 0.2 \text{ nm}$  for high-resolution spectra (577–584 nm range). The spectral resolution of the Raman spectrum is  $\pm 2 \text{ cm}^{-1}$ . The emission decay curves were measured using as the excitation source the second harmonic (at 532 nm) of the fundamental radiation of a Quanta System pulsed Nd-YAG laser. The emission radiation was dispersed with the above mentioned monochromator and detected with a Hamamatsu GaAs photomultiplier connected to a Le Croy Waverunner 500 MHz digital oscilloscope. All the spectroscopic measurements were performed at room temperature.

### 3. RESULTS AND DISCUSSION

The X-ray diffraction pattern of the  $\text{Nb}_2\text{O}_5\text{:Eu}$  sample is reported in Figure 1 as data points, together with the result of the Rietveld fit (full lines). It is possible to assess that the sample is single phase. The pattern is typical of an orthorhombic  $\text{Nb}_2\text{O}_5$  structure, reported with space group  $Pbam$  by Kato and Tamura [13]. The values of lattice parameters refined from the pattern (see Table 1) are not too different from the

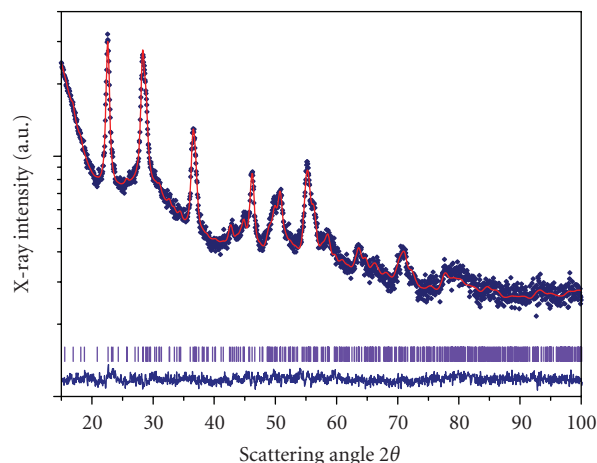


FIGURE 1: XRD patterns for the  $\text{Eu}^{3+}$  doped nanocrystalline  $\text{Nb}_2\text{O}_5$  sample. Dots are experimental data points, full lines are the result of the Rietveld fit. The sequence of bars is calculated from the orthorhombic structure factor  $Pbam$  with the lattice parameters reported in Table 1 and marks the positions expected for any peak. The band at the very bottom of the plot reports the residuals, that is, the difference between the square root of calculated and experimental intensities.

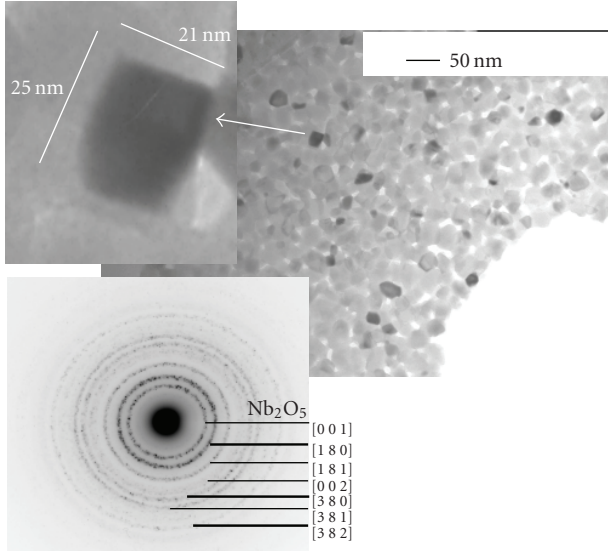
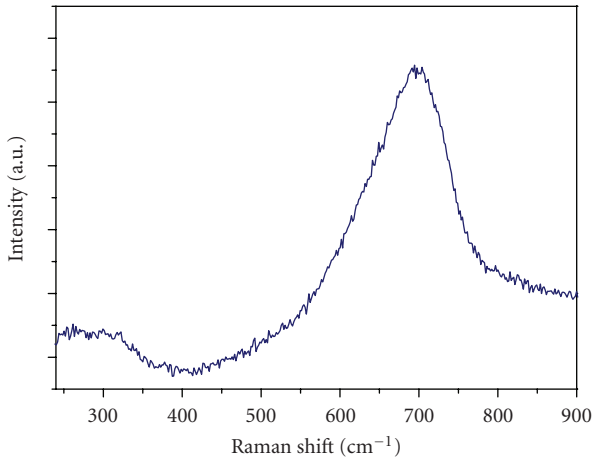
values reported by Kato and Tamura [13] from single crystal data and the small differences found may be ascribed to the insertion into the matrix of the doping agent here used. It should also be noted that various forms of the  $\text{Nb(V)}$  oxide are known from literature, namely tetragonal [14] and monoclinic [15]. Further, additional monoclinic forms exist, which are modified by pressure and temperature. The pattern of our orthorhombic  $\text{Nb}_2\text{O}_5\text{:Eu}$  sample is in close agreement with that reported by Pinna et al. [16]. Direct evaluation of the line broadening by the Rietveld program MAUD, which includes the correction for the instrument function, gives an average crystallite size of about 25 nm with a sensible amount of lattice strain of 0.002.

The crystallography and morphology of the powder were also probed by selected Area electron Diffraction (SAD). In Figure 2(a), a TEM bright field image shows monodisperse rectangular nanoparticles with a narrow particle size distribution. The mean particle dimensions were determined by averaging over about one hundred particles. The average length and width were observed to be 26 and 19 nm, respectively. This result agrees with the size obtained from XRD with the Rietveld method and with the observations by Pinna et al. [16].

The Raman spectrum of the niobia sample under investigation is shown in Figure 3. A strong broad band peaking at about  $700 \text{ cm}^{-1}$  dominates the Raman spectrum although some weaker features around  $300 \text{ cm}^{-1}$  can be observed. The spectrum is very similar to the one found by Brayner and Bozon-Verduraz for a nanocrystalline orthorhombic  $\text{Nb}_2\text{O}_5$  sample prepared by a soft chemical route [17]. The broad band around  $700 \text{ cm}^{-1}$  can be attributed to the stretching modes of the  $\text{NbO}_6$  polyhedra typical of the orthorhombic

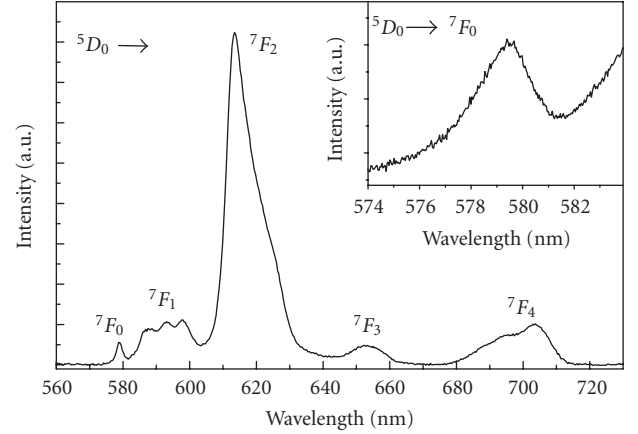
TABLE 1: The main crystallographic and microstructure parameters for the  $\text{Nb}_2\text{O}_5:\text{Eu}$  sample from the best-fit data of Figure 1.

Geometry and space group	Lattice parameters (Å)	Crystallite size (Å)	Lattice strain ( $\times 10^{-3}$ )	Agreement index $R_{\text{wp}}$
Orthorhombic $Pbam$	a = 6.191 ( $\pm 2$ ) b = 29.244 ( $\pm 5$ ) c = 3.926 ( $\pm 2$ )	230 $\pm$ 30	2.0 ( $\pm 0.2$ )	4.7 %

FIGURE 2: TEM and SAD images for the  $\text{Eu}^{3+}$  doped nanocrystalline  $\text{Nb}_2\text{O}_5$  sample.FIGURE 3: Room temperature Raman spectrum of the  $\text{Eu}^{3+}$  doped nanocrystalline  $\text{Nb}_2\text{O}_5$  sample.

$\text{Nb}_2\text{O}_5$  crystalline structure. The remarkable broadening of this band suggests the presence of distorted niobia polyhedra. Besides, the weaker bands around  $300\text{ cm}^{-1}$  are characteristic of the bending modes of the Nb–O–Nb linkages [17].

The room temperature laser excited luminescence spectrum in the 560–730 nm region is shown in Figure 4. The spectrum is characterised by emission bands ascribed to

FIGURE 4: Room temperature luminescence spectrum of the  $\text{Eu}^{3+}$  doped nanocrystalline  $\text{Nb}_2\text{O}_5$  sample ( $\lambda_{\text{exc}} = 488.0\text{ nm}$ ). Inset:  ${}^5D_0 \rightarrow {}^7F_0$  emission band.

${}^5D_0 \rightarrow {}^7F_J$  ( $J = 0, 1, 2, 3, 4$ ) transitions. These bands appear to be significantly broadened, a behaviour typical of lanthanide impurities in disordered environments. It should be noted that the  ${}^5D_0 \rightarrow {}^7F_0$  emission band of the  $\text{Eu}^{3+}$  ion (shown in the inset of Figure 4) is characterised by a full width at half maximum (FWHM) of  $32 \pm 2\text{ cm}^{-1}$ , which is much higher than for ordered crystalline materials, in agreement with the presence of a high degree of disorder for the  $\text{Eu}^{3+}$  sites in the  $\text{Nb}_2\text{O}_5$  host. This FWHM value results to be even higher than the one observed for  $\text{Eu}^{3+}$  doped strontium barium niobate (SBN) single crystals (FWHM =  $24\text{ cm}^{-1}$ ) [6], which are among the crystals affected by a high degree of intrinsic disorder. Moreover, the FWHM for the  $\text{Nb}_2\text{O}_5:\text{Eu}$  sample is very similar to that found for  $\text{Eu}^{3+}$  doped SBN nanocrystalline powders (FWHM of about  $30\text{ cm}^{-1}$ ) [18]. The presence of such disorder is attributed to the difference in the ionic radii in octahedral coordination for  $\text{Nb}^{5+}$  (78 pm) and for  $\text{Eu}^{3+}$  (108.7 pm) [19], so that the substitution of the dopant ion cannot easily occur without distortions, which are likely to be affected by a site-to-site variation. Moreover, the necessary charge compensation could also occur in a variety of different ways, giving rise to a distribution of possible sites for the  $\text{Eu}^{3+}$  ions.

The asymmetry ratio

$$R = \frac{I({}^5D_0 \rightarrow {}^7F_2)}{I({}^5D_0 \rightarrow {}^7F_1)} \quad (1)$$

of the integrated intensities of the hypersensitive  ${}^5D_0 \rightarrow {}^7F_2$  and the magnetic dipole  ${}^5D_0 \rightarrow {}^7F_1$  transitions can be considered indicative of the asymmetry of the coordination

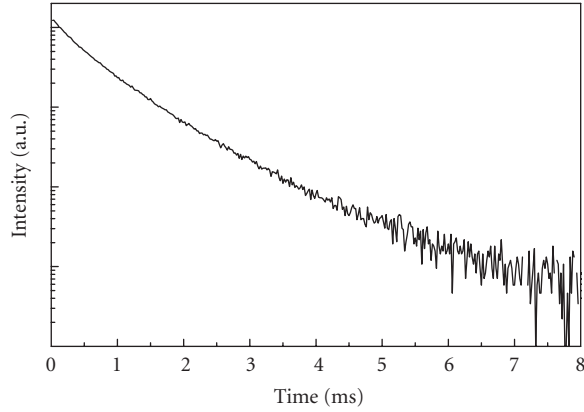


FIGURE 5: Room temperature luminescence decay curve of the  $\text{Eu}^{3+}$  doped nanocrystalline  $\text{Nb}_2\text{O}_5$  sample ( $\lambda_{\text{exc}} = 532 \text{ nm}$ ,  $\lambda_{\text{em}} = 610 \text{ nm}$ ).

polyhedron of the  $\text{Eu}^{3+}$  ion [20]. In particular, the lower the  $R$  value is, the higher is the site symmetry at the  $\text{Eu}^{3+}$  ion. The value of the asymmetry parameter for the  $\text{Nb}_2\text{O}_5:\text{Eu}$  sample, obtained from the measured emission spectra (see Figure 4), results to be  $6.0 \pm 0.1$ . This value indicates that the  $\text{Eu}^{3+}$  ions are accommodated in noncentrosymmetric sites [20], in agreement with the fact that the forbidden transition is clearly detectable. This value appears to be on the upper side of the  $R$  range commonly found for  $\text{Eu}^{3+}$  doped glass hosts ( $R = 3 - 6$ ) [20].

The RT emission decay curve of the  ${}^5D_0$  level (see Figure 5) show a nonexponential behaviour. The nonexponential shape of the luminescence decay curve is mainly ascribed to the disorder affecting the sites in which the  $\text{Eu}^{3+}$  ions are accommodated, as also evidenced by the significant inhomogeneous broadening of the emission bands. We evaluate the effective average emission decay time  $\tau_{\text{avg}}$  using the equation (see [21])

$$\tau_{\text{avg}} = \frac{\int tI(t)dt}{\int I(t)dt}, \quad (2)$$

where  $I(t)$  represents the luminescence intensity at time  $t$  corrected for the background and the integrals are evaluated on a range  $0 < t < t^{\text{max}}$ , where  $t^{\text{max}} \gg \tau_{\text{avg}}$ . The obtained  $\tau_{\text{avg}}$  value for the  $\text{Nb}_2\text{O}_5:\text{Eu}$  sample is  $0.78 \pm 0.01$  millisecond. This value of the effective decay time is similar to that found for SBN nanopowders (about 0.70 millisecond) [18]. The radiative lifetime  $\tau_R$  of the  ${}^5D_0$  level of the  $\text{Eu}^{3+}$  ion can be estimated using the formula (see [22])

$$\frac{1}{\tau_R} = A_{\text{MD},0} n^3 \left( \frac{I_{\text{tot}}}{I({}^5D_0 \rightarrow {}^7F_1)} \right), \quad (3)$$

where  $n$  is the refractive index of the medium,  $A_{\text{MD},0}$  is the spontaneous emission probability for the  ${}^5D_0 \rightarrow {}^7F_1$  transition in vacuo, and  $I_{\text{tot}}/I({}^5D_0 \rightarrow {}^7F_1)$  is the ratio of the total area of the  $\text{Eu}^{3+}$  emission spectrum to the area of the  ${}^5D_0 \rightarrow {}^7F_1$  band. The refractive index of the  $\text{Nb}_2\text{O}_5$  host is taken as 2.4, as reported for  $\text{Nb}_2\text{O}_5$  thin films [23, 24]. The

$A_{\text{MD},0}$  value is estimated to be  $14.65 \text{ s}^{-1}$  [22]. The radiative lifetime  $\tau_R$  of the  ${}^5D_0$  level of the  $\text{Eu}^{3+}$  ion, obtained from (3) and the measured emission spectrum (see Figure 4), results to be 0.56 millisecond. It is worth noting that the experimental effective lifetime  $\tau_{\text{avg}}$  results to be longer than the radiative lifetime obtained from (3). The lengthening of the emission decay time of the  ${}^5D_0$  level was also observed for some  $\text{Eu}^{3+}$  doped nanosized materials, such as  $\text{Eu}^{3+}$  doped  $\text{Y}_2\text{O}_3$  nanopowders [25] and  $\text{Eu}^{3+}$  doped nanocrystalline zirconia [26]. This behavior can be due to a lower refractive index ( $n_{\text{eff}}$ ) surrounding the  $\text{Eu}^{3+}$  ion in the nanocrystalline material with respect to the bulk size host, due to the fact that the filling factor (the fraction of the volume of the host occupied by the nanoparticles) is lower than one [25].

## 4. CONCLUSIONS

This work has shown that the synthesis of nanocrystalline niobia activated with  $\text{Eu}^{3+}$  ions is successfully achieved with the Pechini method. The obtained materials are single phase, with rectangular cross section nanoparticles of crystallite average length and width of 26 and 19 nm. Among the possible niobia polymorphs, the orthorhombic one with space group *Pbam* is observed. The luminescence features are affected by sizeable inhomogeneous broadening due to disorder around the dopant ions. The strongest emission band of the  $\text{Eu}^{3+}$  doped nanocrystalline  $\text{Nb}_2\text{O}_5$  sample peaks at about 610 nm, suggesting a possible use of the present material as a red phosphor for lighting devices. In fact, the emission is quite efficient with reasonably long decay times, also due to the relatively low phonon cutoff of the niobia lattice (about  $700 \text{ cm}^{-1}$ ), making nonradiative relaxation inefficient. Therefore, it appears justified concluding that nanocrystalline  $\text{Nb}_2\text{O}_5$  activated with  $\text{Eu}^{3+}$  ions can be considered as an interesting and promising luminescent and multifunctional material. The present study shows that pentavalent niobium ions can be substituted by trivalent lanthanide ions in crystalline niobates. This substitution is accompanied by a strong disorder around the  $\text{Ln}^{3+}$  ions.

## ACKNOWLEDGMENTS

The authors gratefully acknowledge Erica Viviani (DST, University of Verona) for expert technical assistance and H. C. Starck (GmbH) for kindly providing the niobium ammonium oxalate reagent. Thanks are also expressed to Dr. Luca Lutterotti (<http://www.ing.unitn.it/~luttero>) for making available a copy of the program MAUD running on a personal computer.

## REFERENCES

- [1] D. Hreniak, W. Streck, A. Speghini, M. Bettinelli, G. Boulon, and Y. Guyot, "Infrared induced red luminescence of  $\text{Eu}^{3+}$ -doped polycrystalline  $\text{LiNbO}_3$ ," *Applied Physics Letters*, vol. 88, Article ID 161118, 3 pages, 2006.
- [2] T. Imai, S. Yagi, H. Yamazaki, and M. Ono, "Effects of heat treatment on photorefractive sensitivity of Ce- and

- Eu-doped strontium barium niobate,” *Japanese Journal of Applied Physics*, vol. 38, no. 4A, part 1, pp. 1984–1988, 1999.
- [3] M. O. Ramirez, D. Jaque, L. E. Bausá, J. García-Solé, and A. A. Kaminskii, “Coherent light generation from a Nd:SBN non-linear laser crystal through its ferroelectric phase transition,” *Physical Review Letters*, vol. 95, no. 26, Article ID 267401, 4 pages, 2005.
- [4] A. Yoshikawa, H. Itagaki, T. Fukuda, et al., “Synthesis, crystal growth and second harmonic generation properties of trivalent rare-earth-doped non-linear tungsten-bronze-type structure  $Ba_2Na_{1-3x}RE_xNb_5O_{15}$  (RE = Sc, Y, La, Gd, Yb and Lu),” *Journal of Crystal Growth*, vol. 247, no. 1-2, pp. 148–156, 2003.
- [5] A. Lorenzo, H. Jaffrezic, B. Roux, G. Boulon, and J. García-Solé, “Lattice location of rare-earth ions in  $LiNbO_3$ ,” *Applied Physics Letters*, vol. 67, no. 25, pp. 3735–3737, 1995.
- [6] M. Bettinelli, A. Speghini, A. Ródenas, et al., “Luminescence of lanthanide ions in strontium barium niobate,” *Journal of Luminescence*, vol. 122-123, pp. 307–310, 2007.
- [7] M. O. Ramirez, L. E. Bausá, A. Speghini, M. Bettinelli, L. Ivleva, and J. García-Solé, “Thermal hysteresis in the luminescence of  $Yb^{3+}$  ions in  $Sr_{0.6}Ba_{0.4}Nb_2O_6$ ,” *Physical Review B*, vol. 73, no. 3, Article ID 035119, 8 pages, 2006.
- [8] O. Friedrichs, J. C. Sánchez-López, C. López-Cartes, T. Klassen, R. Bormann, and A. Fernández, “ $Nb_2O_5$  “pathway effect” on hydrogen sorption in Mg,” *Journal of Physical Chemistry B*, vol. 110, no. 15, pp. 7845–7850, 2006.
- [9] T. Hyodo, J. Ohoka, Y. Shimizu, and M. Egashira, “Design of anodically oxidized  $Nb_2O_5$  films as a diode-type  $H_2$  sensing material,” *Sensors and Actuators B*, vol. 117, no. 2, pp. 359–366, 2006.
- [10] M. Kakihana, ““Sol-gel” preparation of high temperature superconducting oxides,” *Journal of Sol-Gel Science and Technology*, vol. 6, no. 1, pp. 7–55, 1996.
- [11] H. M. Rietveld, “Line profiles of neutron powder-diffraction peaks for structure refinement,” *Acta Crystallographica*, vol. 22, part 1, pp. 151–152, 1967.
- [12] L. Lutterotti and S. Gialanella, “X-ray diffraction characterization of heavily deformed metallic specimens,” *Acta Materialia*, vol. 46, no. 1, pp. 101–110, 1998.
- [13] K. Kato and S. Tamura, “Die Kristallstruktur von  $T - Nb_2O_5$ ,” *Acta Crystallographica B*, vol. 31, part 3, pp. 673–677, 1975.
- [14] W. Mertin, S. Andersson, and R. Gruehn, “Über die Kristallstruktur von  $M - Nb_2O_5$ ,” *Journal of Solid State Chemistry*, vol. 1, no. 3-4, pp. 419–424, 1970.
- [15] K. Kato, “Structure refinement of  $H - Nb_2O_5$ ,” *Acta Crystallographica B*, vol. 32, part 3, pp. 764–767, 1976.
- [16] N. Pinna, M. Antonietti, and M. Niederberger, “A novel non-aqueous route to  $V_2O_3$  and  $Nb_2O_5$  nanocrystals,” *Colloids and Surfaces A*, vol. 250, no. 1–3, pp. 211–213, 2004.
- [17] R. Brayner and F. Bozon-Verduraz, “Niobium pentoxide prepared by soft chemical routes: morphology, structure, defects and quantum size effect,” *Physical Chemistry Chemical Physics*, vol. 5, no. 7, pp. 1457–1466, 2003.
- [18] M. Daldosso, A. Speghini, P. Ghigna, et al., “Lanthanide doped strontium barium niobate: optical spectroscopy and local structure at the impurity sites,” to appear in *Journal of Alloys and Compounds*.
- [19] <http://www.webelements.com/>.
- [20] R. Reisfeld, E. Zigansky, and M. Gaft, “Europium probe for estimation of site symmetry in glass films, glasses and crystals,” *Molecular Physics*, vol. 102, no. 11-12, pp. 1319–1330, 2004.
- [21] E. Nakazawa, “Fundamentals of luminescence,” in *Phosphor Handbook*, S. Shionoya and W. M. Yen, Eds., p. 104, CRC Press, Boca Raton, Fla, USA, 1999.
- [22] M. H. V. Werts, R. T. F. Jukes, and J. W. Verhoeven, “The emission spectrum and the radiative lifetime of  $Eu^{3+}$  in luminescent lanthanide complexes,” *Physical Chemistry Chemical Physics*, vol. 4, no. 9, pp. 1542–1548, 2002.
- [23] K. Kukli, M. Ritala, M. Leskelä, and R. Lappalainen, “Niobium oxide thin films grown by atomic layer epitaxy,” *Chemical Vapor Deposition*, vol. 4, no. 1, pp. 29–34, 1998.
- [24] R. Romero, J. R. Ramos-Barrado, F. Martin, and D. Leinen, “ $Nb_2O_5$  thin films obtained by chemical spray pyrolysis,” *Surface and Interface Analysis*, vol. 36, no. 8, pp. 888–891, 2004.
- [25] R. S. Meltzer, S. P. Feofilov, B. Tissue, and H. B. Yuan, “Dependence of fluorescence lifetimes of  $Y_2O_3:Eu^{3+}$  nanoparticles on the surrounding medium,” *Physical Review B*, vol. 60, no. 20, pp. R14012–R14015, 1999.
- [26] A. Speghini, M. Bettinelli, P. Riello, S. Bucella, and A. Benedetti, “Preparation, structural characterization, and luminescence properties of  $Eu^{3+}$ -doped nanocrystalline  $ZrO_2$ ,” *Journal of Materials Research*, vol. 20, no. 10, pp. 2780–2791, 2005.